

# Bulk evidence for single-gap $s$ -wave superconductivity in the intercalated graphite superconductor $C_6Yb$

Mike Sutherland<sup>1</sup>, Nicolas Doiron-Leyraud<sup>2</sup>, Louis Taillefer<sup>2,3</sup>, Thomas Weller<sup>4</sup>, Mark Ellerby<sup>4</sup>, S.S. Saxena<sup>1</sup>

<sup>1</sup>*Cavendish Laboratory, University of Cambridge, J.J. Thomson Ave, Cambridge CB3 0HE, UK*

<sup>2</sup>*Regroupement Québécois sur les Matériaux de Pointe,*

*Département de physique, Université de Sherbrooke, Sherbrooke, Québec, Canada*

<sup>3</sup>*Canadian Institute for Advanced Research, Toronto, Ontario, Canada*

<sup>4</sup>*Department of Physics and Astronomy, University College London, Gower Street, London, UK*

We report measurements of the in-plane electrical resistivity  $\rho$  and the thermal conductivity  $\kappa$  of the intercalated graphite superconductor  $C_6Yb$  to temperatures as low as  $T_c/100$ . When a field is applied along the  $c$ -axis, the residual electronic linear term  $\kappa_0/T$  evolves in an exponential manner for  $H_{c1} < H < H_{c2}$ . This activated behaviour establishes the order parameter as unambiguously  $s$ -wave, and rules out the possibility of multi-gap or unconventional superconductivity in this system.

PACS numbers: 74.70.Wz, 74.25.Fy, 74.25.Op

Carbon is a remarkably versatile element – in its pure form it may exist as an electronic insulator, semiconductor or semimetal depending on its bonding arrangement. When dopant atoms are introduced, superconductivity may be added to this list, observed in graphite [1, 2], fullerenes [3] and even diamond [4]. Superconductivity in doped carbon was first discovered in the graphite intercalate compounds (GICs), materials composed of sheets of carbon separated by layers of intercalant atoms. The first of these compounds were intercalated with alkali atoms, and had modest transition temperatures of 0.13-0.5 K [1]. The recent discovery of  $T_c$ 's two orders of magnitude higher than this in  $C_6Yb$  [5] and  $C_6Ca$  [5, 6] has however refocused attention on this intriguing family of compounds.

The effects of the intercalant atoms in the GICs are two-fold: they dramatically change the electronic properties of the host graphite lattice by both increasing the separation of the carbon sheets, as well as contributing charge carriers. This causes the two-dimensional graphite  $\pi^*$  bands to dip below the Fermi level. The graphite interlayer band, previously unoccupied, also crosses the new Fermi level, contributing three dimensional, free-electron like states located between the carbon sheets. This new interlayer band hybridises strongly with the  $\pi^*$  bands, and its occupation appears to be linked with the occurrence of superconductivity in the GICs [7].

There are still several fundamental questions remaining about superconductivity in the GICs, especially in  $C_6Yb$  and  $C_6Ca$ , where little experimental data exists. The pairing mechanism is unresolved, with speculation ranging from a conventional route involving the intercalant phonons [8, 9, 10] to superconductivity via acoustic plasmons [7].

Early theoretical studies motivated by the alkali-metal GICs [11, 12] emphasized a two-gap model for the superconducting state. In this picture, superconductivity arises from coupling between intercalant  $s$  electrons and the graphite  $\pi$  electrons bands, with gaps of different magnitudes existing on different sheets of the Fermi

surface. Such a scenario is plausible, as there are notable similarities between the GICs and  $MgB_2$  [7, 13], a known multi-gap superconductor. Indeed, some aspects of graphite intercalate superconductivity can be understood by this two-gap phenomenology, however there is little direct evidence to support this picture.

The experimental starting point for addressing these issues is to establish the superconducting order parameter. In  $C_6Yb$  and  $C_6Ca$ , this task is complicated by the difficulties in materials preparation arising from the standard vapour transport process used for intercalation. This process typically yields samples which have a shell of fully intercalated material surrounding a core of unintercalated graphite. In addition, both compounds are extremely sensitive to air, and their surfaces rapidly deteriorate if left exposed. A recent study of penetration depth [14] on  $C_6Ca$  suggested that the superconductivity was  $s$ -wave, however this technique is extremely surface sensitive, and the results were dependent on surface treatment. With these considerations in mind, we turn to measurements of bulk thermodynamic properties to probe the superconducting state.

The technique of thermal conductivity is ideally suited to the study of these materials. It is sensitive only to delocalized states, and in highly conductive systems such as  $C_6Yb$  the majority of the heat transport at low temperatures is provided by electrons, allowing us to easily separate out electronic and phononic contributions to the heat current. Most importantly, thermal conductivity is a *bulk* probe, only marginally affected by small concentrations of impurity phases.

In this Letter we report measurements of low temperature thermal conductivity ( $\kappa$ ) in  $C_6Yb$ , which we use to establish the nature of the superconducting order parameter. The behaviour of  $\kappa$  as the superconducting state is suppressed with a magnetic field shows an activated dependence, clear evidence of  $s$ -wave superconductivity with a single gap energy scale.

Thermal transport was measured down to 60 mK in a dilution refrigerator using a one heater, two thermometer

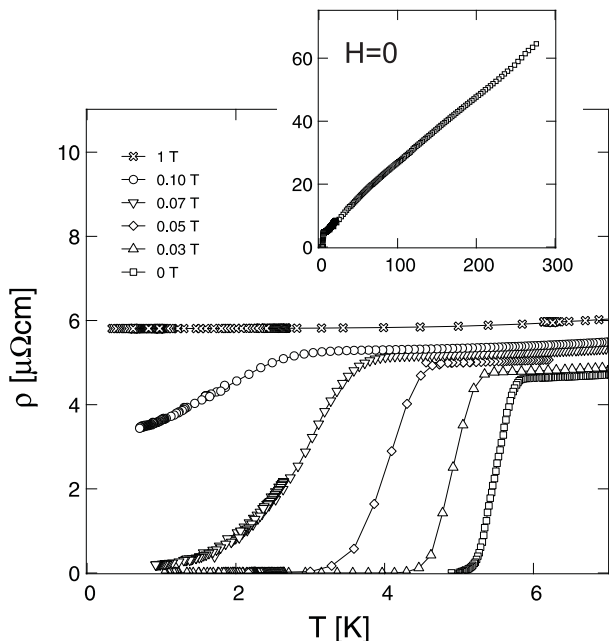


FIG. 1: In plane resistivity for  $C_6Yb$  with  $H \parallel c$ . For  $H = 0$  T the superconducting transition is sharp with  $T_c = 5.4 \pm 0.4$  K but broadens with applied field. For  $H = 1$  T superconductivity is entirely suppressed, revealing a metallic normal state with a residual resistivity  $\rho_0 = 5.8 \mu\Omega\text{cm}$ .

steady state technique. Magnetic fields from 0 to 1 T were applied parallel to the  $c$ -axis and perpendicular to the in-plane heat current. For measurements of  $\kappa(T)$  at constant field, the sample was cooled in field from  $T > T_c$  to maximize homogeneity of the vortex lattice.

Our samples were prepared by intercalating very pure highly oriented pyrolytic graphite (HOPG) using the vapour transport process described elsewhere [5]. In order to obtain samples consisting mainly of intercalated material, we first cleaved the graphite along the  $ab$ -plane, and then took thin bars from the sides. The resulting samples were rectangular platelets of dimensions approximately  $1 \text{ mm} \times 0.5 \text{ mm} \times 100 \mu\text{m}$ . Good quality electrical contacts were made using Dupont silver paint applied directly on the surface after cleaving, with all handling and mounting done in a glove box under flowing He in order to preserve the quality of the samples.

Figure 1 shows the in-plane resistivity of  $C_6Yb$  in both zero field (inset) and as a function of field applied along the  $c$ -axis (main panel). The residual resistivity  $\rho_0$ , is observed to be  $4.5 \mu\Omega\text{cm}$  by extrapolating the zero field curve, and slightly larger than this using the 1 T curve. The magnetoresistance is comparatively weak in  $C_6Yb$  [15], only 30 % by 1 T at 4 K, compared to a factor of 100 increase by only 0.2 T in pure graphite at  $T = 5$  K [16]. From the magnitude of  $\rho_0$  we may estimate the electronic mean free path  $\ell_e$ , assuming  $k_F \sim 0.5 \text{ \AA}^{-1}$  [11] we get  $\ell_e \simeq 1000 \text{ \AA}$  at low temperatures in zero field.

Figure 2 shows the dependence of the thermal conductivity on field for  $H \parallel c$ -axis. By plotting  $\kappa/T$  vs.  $T$

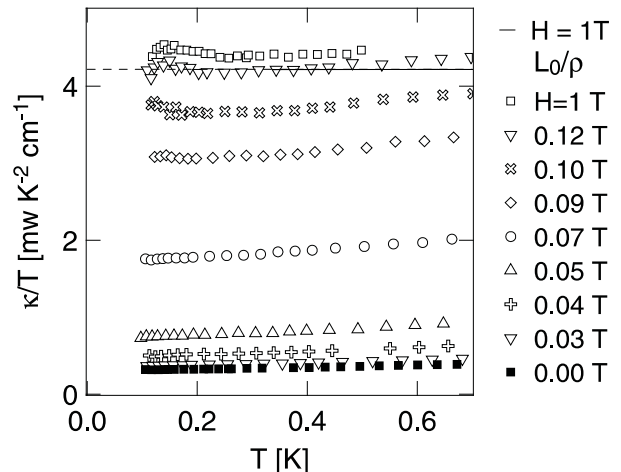


FIG. 2: Low temperature  $\kappa$  of  $C_6Yb$  as a function of applied field, with  $\mathbf{J} \parallel ab$  and  $H \parallel c$ . The black line is the normal state Wiedemann-Franz law expectation estimated from the resistivity in  $H = 1$  T.

we see that  $\kappa/T$  is almost constant, reflecting a dominant electronic contribution. Phonons are responsible for the small slope, which has negligible impact of the field dependence of the residual linear term, the subject of this paper. The rise in  $\kappa$  with  $H$  is gradual at first, then rapidly approaches the normal state value as  $H_{c2}$  is reached. By 1 T the sample is fully in the normal state, and a comparison to the electrical resistivity via the Wiedemann-Franz law is shown by the dashed line. In the normal state we see that this law is obeyed to within 5 %, as expected for a metal in the elastic scattering regime.

Extrapolating the zero field data to  $T = 0$  in Fig.2 yields a small residual linear term  $\kappa_0/T \simeq 0.3 \text{ mWK}^{-2}\text{cm}^{-1}$ . It is tempting to attribute this as arising from nodal quasiparticles in the superconducting state [17], as observed for example in  $d$ -wave superconductors such as the high- $T_c$  cuprates, where  $\kappa_0/T = 1.41 \text{ mWK}^{-2}\text{cm}^{-1}$  for overdoped Tl-2201 with  $T_c = 15$  K [18]. An estimate of the magnitude of the linear term however makes this scenario unlikely. In a nodal superconductor the size of  $\kappa_0/T$  is determined by ratio of the quasiparticle velocities parallel ( $v_2$ ) and perpendicular ( $v_F$ ) to the Fermi surface near the nodes [17]. In a two dimensional  $d$ -wave superconductor with a gap maximum  $\Delta_0$  and a density of  $n$  planes per unit cell of height  $c$  we may write

$$\frac{\kappa_0}{T} = \frac{k_B^2}{6} \frac{n}{d} k_F \left( \frac{v_F}{\Delta_0} \right) \quad (1)$$

assuming  $v_F \gg v_2$  [19]. Using an average  $v_F \simeq 3.4 \times 10^7 \text{ cm/s}$  [12],  $k_F \sim 0.5 \text{ \AA}^{-1}$  [11] and  $\Delta_0 = 2.14 k_B T_c = 1.2 \text{ meV}$  we expect  $\kappa_0/T = 6.1 \text{ mWK}^{-2}\text{cm}^{-1}$  for this system. This is over an order of magnitude larger than what we measure, and on this basis we rule out an uncon-

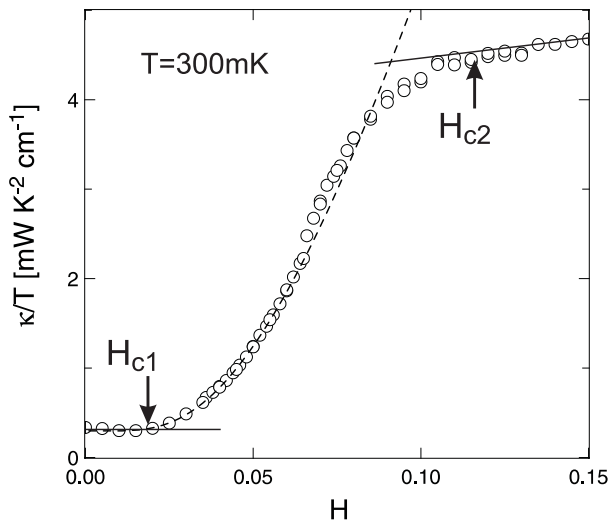


FIG. 3: Thermal conductivity of  $C_6Yb$  at  $T = 300\text{mK}$  as a function of applied field.  $H_{c1}$  and  $H_{c2}$  are determined as the points where the conductivity deviates from a nearly flat  $H$  dependence at low and high fields respectively. The dotted line is a fit to the expected behaviour for an  $s$ -wave superconductor between  $H_{c1} < H < H_{c2}/2$  [21].

ventional order parameter in  $C_6Yb$ . We instead interpret the finite  $\kappa_0/T$  as arising from inclusions of pure graphite where full intercalation was not successful. The extrinsic origin of the linear term is supported by the fact that in a second sample with a similar residual resistivity ( $\rho_0 = 4.4 \mu\Omega\text{cm}$ ),  $\kappa_0/T$  was seen to be half as large.

Since thermal conductivity probes the bulk of a sample, we may use  $\kappa$  as a robust check of the volume fraction of superconducting material. Since an  $s$ -wave superconductor has a fully gapped Fermi surface in the superconducting state, we would expect no contribution to  $\kappa_0/T$  from the intercalated material. The non-intercalated graphite has a residual resistivity of  $\sim 6 \mu\Omega\text{cm}$  [20], and so conducts heat and charge with the same ability as bulk  $C_6Yb$  in the normal state at low temperatures. Thus, the ratio of  $\kappa_0/T$  in the superconducting state to that in the field induced normal state should, to first approximation, yield the volume fraction of non-superconducting graphite inclusions.

Performing this simple analysis yields  $(\kappa_{0,H=0}/T)/(\kappa_{0,H=1T}/T) \simeq 7\%$ , a relatively small fraction of the sample. These arguments demonstrate that good quality, essentially bulk samples of  $C_6Yb$  can be obtained by carefully selecting material from the edges of an intercalated platelet prepared using the vapour transport process.

We now turn to analysing the field dependence of  $\kappa$ . Fig. 3 shows  $\kappa/T(H)$  with  $T$  held constant at 300 mK. Given the small phonon contribution evident from the slope of the data in Fig. 2, the conductivity in the present figure is largely due to electrons. Starting from  $H = 0$  we see that  $\kappa/T$  is close to zero, and essentially flat up to  $H \simeq 0.025$  T with a small conductivity arising from the

non-superconducting graphite regions. For higher fields a sudden increase in  $\kappa/T$  is observed, which we interpret as the onset of the vortex regime at  $H > H_{c1}$ . This agrees reasonably well with estimates of  $H_{c1} = 0.04$  T at low temperatures from magnetization measurements [5].

As the field is further increased, the conductivity evolves in an exponential manner, precisely what is expected for transport in the mixed state of an  $s$ -wave superconductor. As vortices first enter the sample at  $H > H_{c1}$  the only quasiparticle states at  $T \ll T_c$  are those associated within the vortex cores [22]. When the vortices are far apart, these states remain localized, and are unable to contribute to heat transport. Increasing the field decreases the intervortex spacing  $d \sim \sqrt{\Phi_0/B}$  and the states begin to overlap, forming dispersive bands which yield a conductivity that grows exponentially with the ratio of the vortex spacing to the coherence length  $d/\xi$ ,  $\kappa \propto \sqrt{H} \exp(-\alpha \sqrt{H_{c2}/H})$  where  $\alpha$  is a constant. This dependence is readily observed in simple  $s$ -wave superconductors such as Nb [21] for  $H_{c1} < H < H_{c2}/2$ , and is much different than that in nodal superconductors, where the conductivity is observed to increase as  $\sqrt{H/H_{c2}}$  [18]. A fit of our data to the simple  $s$ -wave form is shown Fig. 3, and the good agreement forms the central result of our work: the evolution of the electronic conductivity of  $C_6Yb$  is approximately exponential with applied field, providing the first verification of  $s$ -wave superconductivity in intercalated graphite using a bulk thermodynamic technique.

At still higher fields, the conductivity rolls off and eventually saturates as the sample enters the normal state. From the data in Fig. 3 we estimate this to occur at  $H \simeq 0.12$  T, in good agreement with estimates of  $H_{c2} = 0.11$  T from magnetization measurements [5]. With  $H_{c2}(\parallel c) = 0.12$  T we estimate  $\xi_{ab} \simeq 525 \text{ \AA} \sim \ell_e$ , which places  $C_6Yb$  in the dirty limit. This observation is consistent with the fact that the rise in conductivity with field is not as dramatic as in clean Nb [23], but closely resembles that observed in dirty limit Nb [24] and metal alloy superconductors [25, 26].

In addition to confirming  $s$ -wave superconductivity, the activated behaviour observed in Fig. 3 rules out the scenario of multi-gap superconductivity originally proposed for the GIC's [11]. In Fig. 4 we compare  $C_6Yb$  to other type-II superconductors by plotting the normalized value of  $\kappa_0/T$  versus applied field. The similarity between  $C_6Yb$  and the alloyed superconductor InBi with  $T_c = 4.0$  K and  $H_{c2} = 0.07$  T [25] is striking. Both curves are exponential with field at low  $H$ , crossing over to a roughly linear behaviour closer to  $H_{c2}$  as expected for  $s$ -wave superconductors in the dirty limit [28]. The clean limit case observed in pure Nb [23] is shown for contrast. These three curves are very different from the behaviour of the archetypal multi-band superconductor  $MgB_2$  [27], or the archetypal  $d$ -wave superconductor Tl-2201 [18].

In the multiband scenario, gaps of different magnitudes are associated with the  $\pi$  and  $\sigma$  bands. Such a situation

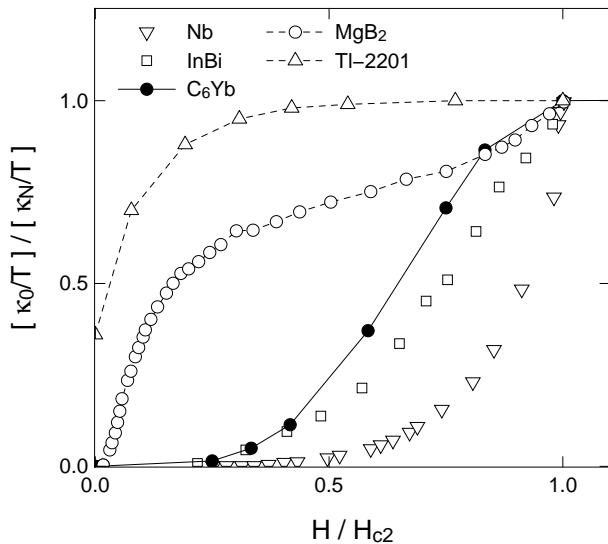


FIG. 4: The normalized residual linear term  $\kappa_0/T$  of sample B plotted as a function of  $H/H_{c2}$ , with the small contribution from graphite impurities subtracted off. For comparison, similar low-temperature data for the clean  $s$ -wave superconductor Nb [23], the dirty  $s$ -wave superconducting alloy InBi [25], the multi-gap superconductor  $MgB_2$  [27] and an over-doped sample of the  $d$ -wave superconductor Tl-2201 [18] are plotted alongside.

is expected for instance when one band has strong pairing and induces superconductivity in the other by Cooper

pair tunnelling [29], or when electron-phonon coupling is significantly different for different bands. Applying a field rapidly delocalizes quasiparticles states confined within the vortices associated with the smaller gap band, while those states associated with the larger gap band delocalize more slowly. This gives rise to the rapid increase in conductivity at low fields and relatively flat dependence at higher fields [30] evident for in the  $MgB_2$  [27] data shown in Fig. 4. Our own data thus allows us to rule out any sizable difference between the size of the gaps associated with each band in  $C_6Yb$ , and suggests a single gap energy scale for the electrons as in the conventional  $s$ -wave scenario.

In summary we have used bulk measurements of the thermal conductivity  $\kappa$  to definitively establish  $s$ -wave superconductivity in  $C_6Yb$ , and rule out an order parameter with nodes. The activated behaviour of  $\kappa_0/T$  also strongly suggests that the pairing state is isotropic, very similar to elementary type-II superconductors in the dirty limit. It will interesting to confirm these results on other members of the intercalate family with complementary techniques, although it seems likely that other GICs will share similar superconducting properties.

We would like to thank Robert Smith, Sibel Özcan and Gil Lonzarich for useful discussions. M.S. and N.D-L acknowledge support from an NSERC of Canada postdoctoral fellowship, and L.T. acknowledges support from a Canada Research Chair. This research was funded by EPSRC, NSERC and the CIAR.

- 
- [1] N. Hannay et al., Phys. Rev. Lett. **14**, 225 (1965).  
[2] Y. Koike et al., Physica B+C **99**, 503 (1980).  
[3] A. Hebard et al., Nature **350**, 600 (1991).  
[4] E. Ekimov et al., Nature **428**, 542 (2004).  
[5] T. E. Weller et al., Nature Physics **1**, 39 (2005).  
[6] N. Emery et al., Phys. Rev. Lett. **95**, 087003 (2005).  
[7] G. Csanyi et al., Nature Physics **1**, 42 (2005).  
[8] I.I. Mazin, Phys. Rev. Lett. **95**, 227001 (2005).  
[9] I.I. Mazin and S. Molodtsov, Phys. Rev. B **72**, 172504 (2005).  
[10] M. Calandra and F. Mauri, Phys. Rev. Lett. **95**, 237002 (2005).  
[11] R. Al-Jishi, Phys. Rev. B **28**, 112 (1983).  
[12] R. A. Jishi and M. S. Dresselhaus, Phys. Rev. B **45**, 12465 (1992).  
[13] P. Konsin and B. Sorkin, Supercond. Sci. Technol. **17**, 1472 (2004).  
[14] G. Lamura et al., Phys. Rev. Lett. **96**, 107008 (2006).  
[15] It is probable that all or most of this magnetoresistance arises from small inclusions of pure graphite, estimate to make up a few percent of our sample in the following paragraphs.  
[16] X. Du, S. Tsai, D. Maslov, and A. Hebard, Phys. Rev. Lett. **94**, 166601 (2005).  
[17] A.C. Durst and P.A. Lee, Phys. Rev. B **62**, 1270 (2000).  
[18] C. Proust, E. Boaknin, R.W. Hill, L. Taillefer, and A.P. Mackenzie, Phys. Rev. Lett. **89**, 147003 (2002).  
[19] D. Hawthorn et al., cond-mat/0502273 (2005).  
[20] D. Morelli and C. Uher, Phys. Rev. B. **30**, R1080 (1984).  
[21] W. Vinen et al., Physica (Amsterdam) **55A**, 94 (1971).  
[22] C. Caroli, P. DeGennes, and J. Matricon, Phys. Lett. **9**, 307 (1964).  
[23] J. Lowell and J. Sousa, J. Low. Temp. Phys. **3**, 65 (1970).  
[24] S. Wasim and N. Zebouni, Phys. Rev. **187**, 539 (1969).  
[25] J. Willis and D. Ginsberg, Phys. Rev. B **14**, 1916 (1976).  
[26] R. Parks, F. Zumsteg, and J. Mochel, Phys. Rev. Lett. **18**, 47 (1967).  
[27] A. V. Sologubenko, J. Jun, S. Kazakov, J. Karpinski, and H. Ott, Phys. Rev. B **66**, 014504 (2002).  
[28] C. Caroli and M. Cyrot, Phys. Kondens. Mater. **4**, 285 (1965).  
[29] N. Nakai, M. Ichioka, and K. Machida, J. Phys. Soc. Jpn. **71**, 23 (2002).  
[30] H. Kusunose, T.M. Rice, and M. Sigrist, Phys. Rev. B **66**, 214503 (2002).